

Vimentin Binding to Phosphorylated Erk Sterically Hinders Enzymatic Dephosphorylation of the Kinase

Eran Perlson¹, Izhak Michaelovski¹, Noga Kowalsman¹
Keren Ben-Yaakov¹, Maya Shaked¹, Rony Seger²
Miriam Eisenstein³ and Mike Fainzilber^{1*}

¹Department of Biological Chemistry, Weizmann Institute of Science, 76100 Rehovot, Israel

²Department of Biological Regulation, Weizmann Institute of Science, 76100 Rehovot, Israel

³Department of Chemical Research Support, Weizmann Institute of Science 76100 Rehovot, Israel

Cleavage fragments of *de novo* synthesized vimentin were recently reported to interact with phosphorylated Erk1 and Erk2 MAP kinases (pErk) in injured sciatic nerve, thus linking pErk to a signaling complex retrogradely transported on importins and dynein. Here we clarify the structural basis for this interaction, which explains how pErk is protected from dephosphorylation while bound to vimentin. Pull-down and ELISA experiments revealed robust calcium-dependent binding of pErk to the second coiled-coil domain of vimentin, with observed affinities of binding increasing from 180 nM at 0.1 μ M calcium to 15 nM at 10 μ M calcium. In contrast there was little or no binding of non-phosphorylated Erk to vimentin under these conditions. Geometric and electrostatic complementarity docking generated a number of solutions wherein vimentin binding to pErk occludes the lip containing the phosphorylated residues in the kinase. Binding competition experiments with Erk peptides confirmed a solution in which vimentin covers the phosphorylation lip in pErk, interacting with residues above and below the lip. The same peptides inhibited pErk binding to the dynein complex in sciatic nerve axoplasm, and interfered with protection from phosphatases by vimentin. Thus, a soluble intermediate filament fragment interacts with a signaling kinase and protects it from dephosphorylation by calcium-dependent steric hindrance.

© 2006 Elsevier Ltd. All rights reserved.

*Corresponding author

Keywords: vimentin; Erk; phosphorylation; intermediate filament; docking

Introduction

The 42 and 44 kDa extracellular signal regulated kinases (Erk) are critical signaling transducers involved in multiple physiological pathways in eukaryotic cells. Erks are found as nodes in complex signaling networks with multiple inputs and a large variety of interactors, thus the specificity of Erk signaling is dependent on a host of inhibitors, scaffolds and substrates.^{1,2} Subcellular localization and spatial regulation are important aspects of Erk signal determination, for example translocation from the cytoplasm to the nucleus changes the spectrum of available substrates and the downstream consequences of Erk activation.³ Moreover, movement of

activated Erk within the cytoplasm is required for transduction of signal from the cell surface to effectors within the cell and the nucleus. Fidelity of signaling must therefore be dependent on preservation of Erk in its activated form during translocation, or on regeneration of the signal en route.⁴ Indeed, theoretical analyses and quantitative models have suggested that active mechanisms must exist for transport and preservation or regeneration of Erk phosphorylation for signal translocation to occur over distances greater than a few μ m within a cell.^{5,6}

Neurons provide impressive examples of cells requiring signal transduction over distances three to six orders of magnitude greater than the calculated threshold for unassisted movement of a signaling kinase. Different members of the MAP kinase family, including Jnks and Erks, are involved in long distance signaling pathways from axons or dendrites to neuronal cell bodies.^{7–9} One such pathway is the retrograde injury signaling mechanism activated upon lesion of a neuronal process, and acting *via* a

Abbreviations used: PDB, Protein Data Bank; GST, glutathione-S-transferase.

E-mail address of the corresponding author: mike.fainzilber@weizmann.ac.il

macromolecule complex assembled at the lesion site and transported retrogradely to the cell body by dynein motor movement on microtubules.^{10,11} In mammalian peripheral sensory neurons formation of the complex is initiated by local synthesis of the nuclear import factor importin β at the injury site.¹² The newly synthesized importin β links up with importin α constitutively bound to dynein, thus forming a high affinity cargo-binding complex on the retrograde motor. Recently, we have shown that the intermediate filament vimentin is also synthesized *de novo* following axonal injury. Soluble fragments of vimentin are generated concomitantly by calpain-mediated cleavage, and these fragments then bind importin β on the one hand and phosphorylated Erks 1 or 2 (pErk) on the other, thus linking pErk to the retrograde transport complex formed by importins and dynein.^{13,14}

Vimentin linkage of pErk to retrograde transport was also shown to maintain Erk phosphorylation en route.¹⁴ The mechanism for maintenance of phosphorylation is yet unknown, and its elucidation is key to understanding how kinase signaling is propagated over long intracellular distances. Here we investigated the interaction of vimentin with pErk using biochemical and molecular modeling approaches. pErk binding was localized to the second coil-coiled domain of vimentin, but not of peripherin. pErk-vimentin binding was calcium-dependent, with observed affinities of binding increasing from 180 nM at 0.1 μ M calcium to 15 nM at 10 μ M calcium. In contrast there was little or no binding of non-phosphorylated Erk to vimentin under these conditions. A docking model of the pErk-vimentin complex was verified by peptide competition assays and revealed that the structural basis for vimentin protection of pErk is by steric hindrance of access to the phosphorylation lip.

Results and Discussion

Vimentin, like other intermediate filaments, has a three domain structure comprising amino and carboxy-terminal head and tail domains flanking a central α -helical rod domain.^{15–17} The rod domain contains a heptad repeat pattern with short linkers interspersed between two consecutive α -helical segments termed the first and second coiled-coil domains (Figure 1(a)). The head domain is important for filament assembly, while the rod domain was shown to have nuclear localization determinants in the last amino acid residues of the second coiled-coil.¹⁸ The tail contains an element responsible for cytoplasmic retention of vimentin and the proteins that it anchors.^{18,19} In order to understand the interactions of vimentin with pErk, we constructed a number of clones corresponding to structural subdomains of vimentin. Radiolabelled protein products of these constructs were tested in comparative pull-downs *in vitro* with recombinant pErk-GST. The second coiled-coil was the only vimentin subdomain pulled down with pErk on its own, and

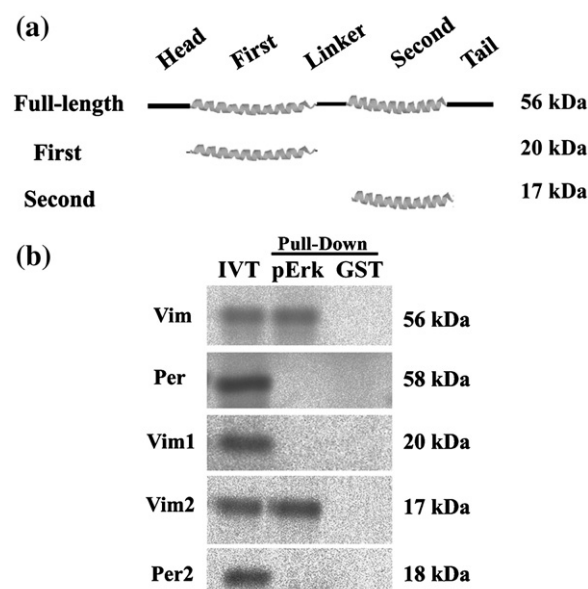


Figure 1. The second coiled coil of vimentin interacts with phosphorylated Erk. (a) Schematic overview of vimentin subdomains and constructs tested. (b) Pull-down of *in vitro* translated vimentin subdomains with pErk. Both full length and the second coiled coil domain of vimentin co-precipitate with pErk, but not the first coiled coil of vimentin or the second coiled coil of peripherin. This experiment was repeated three times with similar results.

other vimentin subdomains or the corresponding subdomain from peripherin did not co-precipitate with pErk (Figure 1(b)). Thus, the main pErk-binding domain in vimentin is within the second coiled coil region in the rod domain. The specificity of the interaction is striking, since the second coiled coils in vimentin and peripherin have highly homologous sequences.

In order to obtain further insight on the pErk-vimentin interaction we generated docking models using the available crystal structures of residues 6–358 of pErk (structure 2ERK in the Protein Data Bank (PDB)) and residues 328–406 of vimentin (PDB structure 1GK4). The kinase structure covers almost the entire molecule, with phosphorylation at residues Thr183 and Tyr185.²⁰ The vimentin structure contains three pairs of coil-coiled fragments, overlapping considerably with the pErk-binding domain identified in Figure 1.²¹ Geometric-electrostatic-hydrophobic docking models were obtained using the MolFit algorithm.²² The top ranking models, with high geometric and electrostatic complementarity, formed the cluster shown in Figure 2(a). In another group of highly ranked models the vimentin molecule interacts with the substrate-binding cavity of pErk (data not shown). In order to discriminate between these two clusters of models we synthesized a series of peptides corresponding to surface-exposed regions in Erk (see Materials and Methods), and tested their effects in competitive displacement assays of vimentin from pErk (Figure 2(b)). Three

distinct peptides were found to interfere with vimentin binding to pErk, corresponding to residues Erk₆₋₂₀, Erk₈₉₋₁₀₃ and Erk₂₂₀₋₂₃₃. These data clearly support the model shown in Figure 2(a) wherein vimentin comes in contact with the kinase at binding sites both above and below the lip containing the phosphorylated residues, fitting on the one side into a groove in between the two sequence regions in the N-terminal domain. The phosphorylated residues of pErk are occluded by vimentin, as also emphasized in Figure 2, which shows the electrostatic complementarity in the final model. Notably, our docking computations clearly identified the interaction site of pErk but not the interaction site of vimentin, probably because of the symmetrical shape of this molecule and its electrostatic potential. Some insight on the vimentin binding site can be obtained by comparing the sequences of vimentin-B2, vimentin-B1 and peripherin. Such comparison suggests that

the stutter region in peripherin is different from in vimentin-B2 and the overall charge of this fragment is smaller. The vimentin B1 fragment does not have a stutter region.

Further support for the proposed mode of vimentin-pErk interaction was obtained in a series of quantitative binding assays. GST-fused Erk or pErk were immobilized in glutathione coated 96-well plates, and then incubated with vimentin and competing peptides before washing and quantification of vimentin binding by ELISA. We first compared vimentin binding to pErk *versus* non-phosphorylated Erk in buffer containing 1 μ M calcium and observed a saturation-binding curve for pErk with an apparent EC₅₀ of 70 nM, with little or no binding for non-phosphorylated Erk (Figure 3(a)). We then performed a series of binding assays

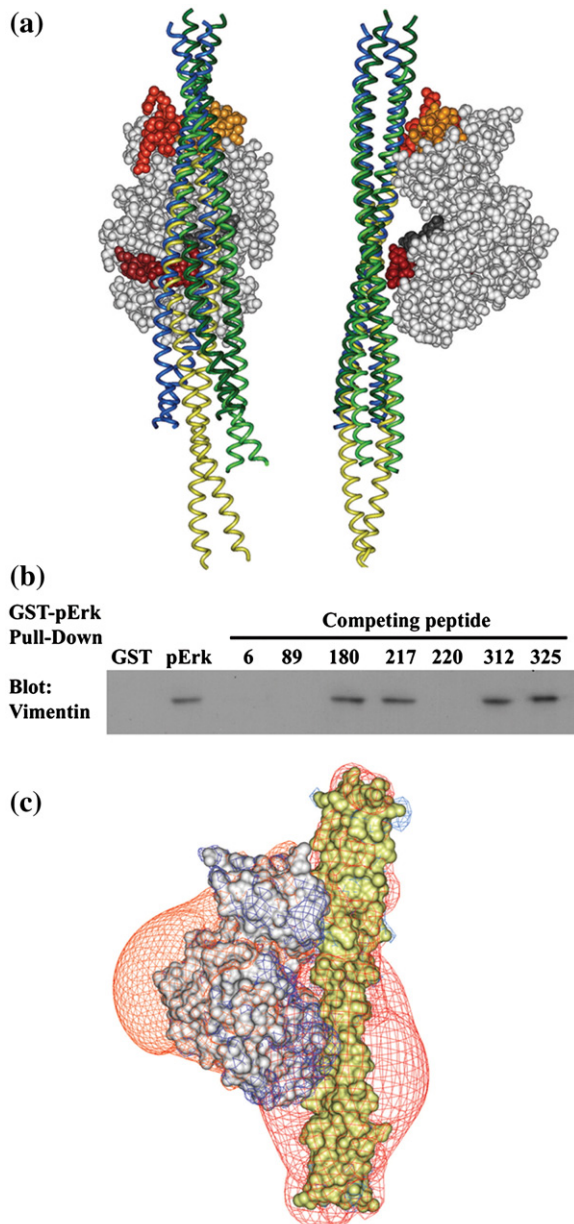


Figure 2. Modeling the pErk-vimentin interaction. (a) Top ranking ensemble of MolFit models with good electrostatic and geometric complementarity. Two views are shown rotated vertically by 90°. The space-filling model of the kinase molecule is shown in light gray with the phosphorylated residues (Thr183 and Tyr185) emphasized in dark grey. The blue, yellow, green and dark green ribbons represent four positions of vimentin in this ensemble; they make very similar interactions with the kinase in the groove between Erk residues 89–103 (golden) and 6–20 (red) but the green models are shifted slightly compared to the blue and yellow models in the vicinity of residues 220–233 (dark red) in Erk (see front view). These three peptides were shown experimentally to disrupt the pErk-vimentin interaction (see (b)). The light green model is shifted with respect to the dark green model along the long axis of the vimentin fragment and rotated about this axis, resulting in good superposition of the helical backbones. These two solutions demonstrate the difficulty to distinguish between docking predictions when a highly symmetrical molecule (shape and electrostatic potential) like the vimentin fragment is docked. Another example of the effect of the vimentin symmetry is demonstrated by the effect of the vimentin symmetry is demonstrated by the yellow model. In this case the vimentin molecule is rotated about an axis perpendicular to its long axis and therefore the C to N direction is reversed compared to the other solutions. The considerable translation along the long axis of the molecule is driven by the electrostatic potential, maximizing the overlap of the negative region of vimentin with the positive region of the kinase at this relative orientation. Note that in the front view the vimentin solutions differ slightly in their interactions with the lower lobe of the kinase, whereas in the side view their positions relative to the kinase are very close. (b) Effects of Erk-derived synthetic peptides on the interaction of vimentin with pErk. The peptides were incubated with vimentin at 20:1 molar ratio for 2 h at room temperature, followed by GST-pErk pull-down. Peptides Erk-6-20, 89-103 and 220-233 clearly inhibit pErk-vimentin binding, thus verifying the blue ribbon solution in (a). This experiment was repeated three times with similar results. (c) Electrostatic complementarity in the proposed model for the interaction between phospho-Erk2 and the vimentin 2B fragment. The solvent accessible surface is shown in gray for the kinase molecule and in yellow for the 2B vimentin fragment. Electrostatic equipotential line-surfaces at ± 1.5 kT/e are shown in orange (negative) and dark blue (positive) for the kinase and in red (negative) and blue (positive) for vimentin 2B.

for the vimentin-pErk interaction under different calcium concentrations, and observed a strong positive effect of calcium on binding affinity, with EC_{50} decreasing from 180 nM at 0.1 μ M calcium to 15 nM at 10 μ M calcium (Figure 3(b)). Finally, we characterized the displacement affinities of the Erk-derived competitor peptides identified in Figure 2(c), and observed a higher affinity for Erk₆₋₂₀ as compared to Erk₈₉₋₁₀₃ or Erk₂₂₀₋₂₃₃ (Figure 3(c)).

Erk, as other kinases, can be rapidly dephosphorylated by a number of phosphatases.³ Since vimentin was previously shown to protect Erk from dephosphorylation,¹⁴ we tested the capacity of the

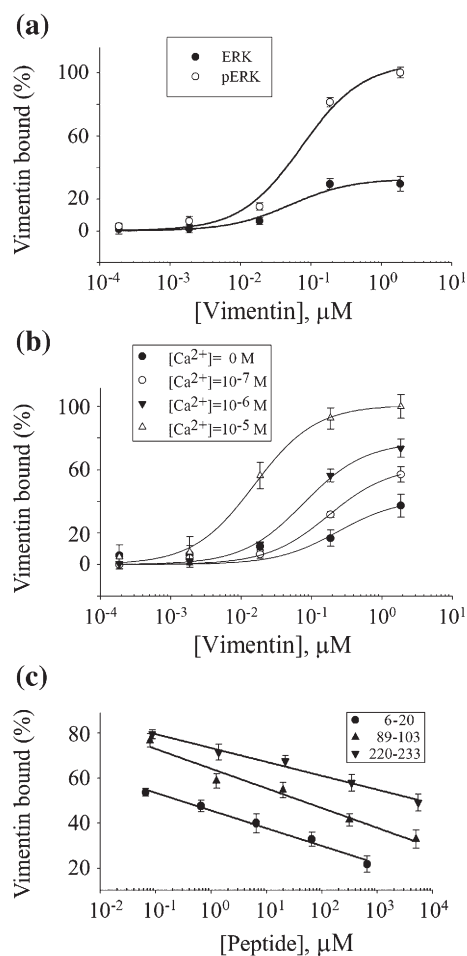


Figure 3. ELISA quantification of pErk-Vimentin binding. (a) Comparison of vimentin binding to immobilized Erk versus pErk reveals significantly enhanced binding upon Erk phosphorylation ($n=4$). (b) Effect of Ca^{2+} levels on vimentin-pErk binding. EC_{50} values calculated from the binding curves are Ca^{2+} 0 M, EC_{50} 0.24(\pm 0.02) μ M; Ca^{2+} 0.1 μ M, EC_{50} 0.18(\pm 0.03) μ M; Ca^{2+} 1 μ M, EC_{50} 80(\pm 8.02) nM; Ca^{2+} 0.1 μ M, EC_{50} 15(\pm 1.85) nM. (c) Competition of Erk-derived peptides with pErk for vimentin binding. Vimentin-peptide premix was applied to immobilized GST-pErk or GST alone in buffer containing 1 μ M Ca^{2+} . The vimentin concentration used was 0.186 μ M, well within the linear range of the vimentin-pErk binding curve. Peptide IC_{50} s deduced from the binding competition data are Erk₆₋₂₀ 0.26(\pm 0.02) μ M; Erk₈₉₋₁₀₃ 10.3(\pm 1.0) μ M; Erk₂₂₀₋₂₃₃ 603.6(\pm 8.02) μ M. All values are average + Std. Error.

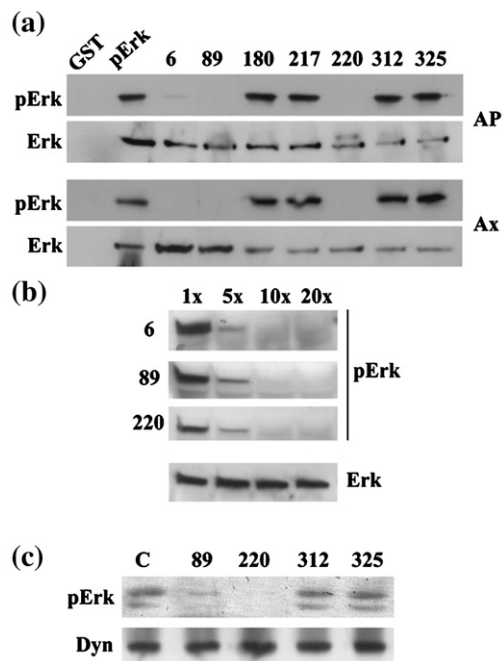


Figure 4. Phosphatase protection of pErk by vimentin. (a) Erk-derived peptides were incubated with vimentin at 20:1 molar ratio peptide:vimentin for 2 h at room temperature. GST-pErk was added and incubated for a further 2 h, calcium was at 1 μ M throughout. Alkaline phosphatase (AP, two units) or axoplasm from injured nerve 6 h post-lesion (Ax, 100 μ g) was added for an additional 30 min before performing GST pull-down followed by Western blotting for pErk and Erk. (b) Dose response analysis for the peptides shown to interfere with phosphatase protection in (a), now applied at molar ratios from 1:1 until 20:1 peptide:vimentin. (c) Effect of selected Erk-derived peptides on co-precipitation of endogenous pErk with dynein from sciatic nerve axoplasm. Sciatic nerves of adult rats were injected with excess amounts of the indicated peptides concomitantly with lesion, and 6 h later 300 μ g aliquots of axoplasm were subjected to dynein immunoprecipitation, followed by Western blot for pErk. All experiments were repeated at least three times with similar results.

displacing peptides identified above to disrupt phosphatase protection. As shown in Figure 4(a), the same peptides that interfere with vimentin-pErk binding antagonize vimentin protection of Erk phosphorylation. Erk was rapidly dephosphorylated by either alkaline phosphatase or by sciatic nerve axoplasm when vimentin binding was competed by peptides Erk₆₋₂₀, Erk₈₉₋₁₀₃ and Erk₂₂₀₋₂₃₃, but not by other Erk-derived peptides (Figure 4(a) and (b)), as would be expected from the docking model. As a final examination of the validity of the model *in vivo*, we tested the ability of selected Erk-derived peptides to disrupt the endogenous complex in injured sciatic nerve by conducting dynein immunoprecipitations followed by Western blots for pErk. Peptides Erk₈₉₋₁₀₃ and Erk₂₂₀₋₂₃₃ both prevented co-precipitation of pErk with dynein from sciatic nerve, while two other Erk-derived peptides that do not target the binding interface had no effect

(Figure 4(c)). Thus, peptide competition experiments are consistent with the proposed mode of vimentin-pErk interaction both *in vitro* using isolated proteins and *in vivo* on the endogenous complex.

The model described in Figure 2 and the biochemical evidence supporting it highlight vimentin as a new type of Erk interactor. Although previous studies have described a wealth of substrates, inhibitors and scaffolds for Erk,³ the mode of vimentin binding to Erk does not seem to fit any of these three categories. Two main regions in Erk have been implicated as docking motifs for the binding of most of the interacting proteins. These are the cytosolic retention sequence/common docking motif (CRS/CD),^{23,24} that interact with D domains in the interacting proteins, and the docking site for Erk (DEF)-docking motif that interacts with FFX motifs.²⁵ Although binding to one of the motifs may be sufficient for a stable interaction, many of the interactions are mediated through both motifs.³ Other docking sites that seem to be less prevalent are the L6 that was shown to interact specifically with microtubules,²⁶ and the N-terminal part of Erk that was shown to interact with MEK.²⁷ Our results here indicate that the binding to vimentin is likely to involve three out of the four interaction motifs, including the N terminus (peptide 6-20) the L6 region (peptide 89-103) and possibly the DEF-docking motif (peptide 220-233). These results support the notion that Erk contains several binding sites that can be used variably to interact with different proteins, and thereby dictate its spatial and temporal regulation. Furthermore, vimentin binding to pErk will likely preclude binding of most other known interactors, thus ensuring no change in Erk activation state as long as vimentin stays bound. Vimentin therefore seems to act as a chaperone-like molecule, protecting Erk from dephosphorylation by occluding the phosphorylation lip and restricting phosphatase access by steric hindrance. This binding mode is particularly suited to the proposed role of the interaction in enabling long distance transport of phosphorylated Erk within the cell.^{14,28,29} Calcium dependence of the interaction provides a switch for binding and release of vimentin from pErk (Figure 3(c)), thus favoring translocation of the Erk signal from high calcium to low calcium conditions in the cell. Future efforts on structure determination of the vimentin-Erk complex at different calcium concentrations may shed light on the details of this switch mechanism. Furthermore it will be intriguing to find out if the described mode of vimentin protection of pErk is recapitulated for other pairs of intermediate filaments and signaling kinases important for long distance transport.

Materials and Methods

Antibodies, proteins and peptides

Antibodies polyclonal anti-Erk M5670 and monoclonal anti-doubly phosphorylated Erk M8159 were both from

Sigma (Rehovot, Israel); monoclonal anti-dynein 74 kDa Intermediate Chain MAB1618, monoclonal anti-Vimentin clone V9 MAB3400 and polyclonal anti-Vimentin AB1620 were all from Chemicon International (Temecula, CA, USA). Recombinant Syrian hamster vimentin was from Cytoskeleton Inc (Denver, CO, USA). The following peptides were synthesized by Ansynth BV (Roosendaal, The Netherlands):

Erk₆₋₂₀, AAGPEMVRGQVFDVG;
 Erk₂₄₋₃₇, TNLSYIGEGAYGMV;
 Erk₈₉₋₁₀₃, RAPTIEQMKDVYIVQ;
 Erk₁₈₀₋₁₉₃, GFLTEYVATRWYRA;
 Erk₂₁₇₋₂₃₀, AEMLSNRPIFPKGK;
 Erk₂₂₀₋₂₃₃, LSNRPIFPKGKHYLD;
 Erk₂₄₀₋₂₅₄, GILGSPSQEDLNCII;
 Erk₂₅₅₋₂₆₈, NLKARNYLLSLPHK;
 Erk₃₁₂₋₃₂₆, EQYYDPSDEPIAEAP;
 Erk₃₂₅₋₃₃₈, APFKFDMELDDLPK.

DNA constructs

Mouse vimentin and peripherin cDNAs were a kind gift from Dr Robert Shoeman (Max Planck Institute for Cell Biology, Rosenhof, Germany). Full-length open reading frames and subdomains were amplified by PCR, subcloned into pCDNA3, and verified by sequencing. Constructs and primer sets were: peripherin, forward primer AAAGAATTCGCCCGTTCATTCCTTTGCT and reverse primer AAAGCGGCCGCTTCTTCATCGCCTCTTCC, cloning sites EcoRI and NotI; second peripherin coiled coil, forward primer CCGGAATTCCTGAGGGACATCCGTGC and reverse primer ATAAGAATGCGGCCGCGCTCTCCTCCCTTCCA, cloning sites EcoRI and NotI; vimentin, forward primer AAAGGATCCATGTCTAC-CAGGTCTGTGTC and reverse primer ACTTCTCAG-CATCACGATGACTCTAGATTT, cloning sites BamHI and XbaI; first vimentin coiled coil, forward primer AAA-GGATCCGGCGTGCGGCTGCTTCAA and reverse primer ACGACGAGGAGATCCAGGAGTCTAGATTT, cloning sites BamHI and XbaI; second vimentin coiled coil, forward primer AAAGGATCCGTGCAGATCGACG-TGGAC and reverse primer ACATCGAGATCGCCACC-TACTCTAGATTT, cloning sites BamHI and XbaI.

Docking and modeling

The structures of pERK and vimentin were obtained from the Protein Data Bank and docked using the program MolFit.²² MolFit treats the molecules as rigid bodies. They are represented by three-dimensional grids in which each grid point carries information concerning its position with respect to the surface/interior of the molecule. The surface grid points carry chemical information such as the electrostatic potential and the hydrophobicity of the surface. MolFit performs an exhaustive scan of the relative rotations and translations of the molecules and produces a list of models evaluated by a geometric-electrostatic-hydrophobic complementarity score.

Recombinant expression of pErk

To obtain doubly phosphorylated Erk, activated human GST-Erk2 was co-expressed with constitutively active MEK1 in BL21 bacteria, as described.³⁰ The bacteria were grown in 2YT medium at 30 °C to an absorbance of 0.6, and then 1 mM IPTG was added for an additional 4 h.

Proteins were purified over Glutathione-Sepharose 4B (Amersham Biosciences) or Nickel-NTA Agarose (Qia- gene) according the manufacturer's instructions.

GST pull-downs and immunoprecipitations

GST-pErk or glutathione-S-transferase (GST) alone were equilibrated in 1 ml nuclear transport buffer (NTB)¹² with 1 μ M calcium, 2 mM PMSE, 2% (w/v) BSA and proteinase inhibitors. [³⁵S]Met/Cys labelled proteins were prepared from DNA constructs by *in vitro* transcription and translation using the TNT coupled reticulocyte lysate system (Promega), according to the manufacturer's instructions. *In vitro* translated protein was added to the GST-pErk or GST and incubated for 2 h at 37 °C before pull-down on glutathione-Sepharose beads. Beads were washed twice with 0.2 M NaCl in NTB and twice again with NTB before elution in SDS-PAGE sample buffer for loading on gels. Dynein co-immunoprecipitations and Western blots for vimentin were performed as described.¹⁴

Phosphatase protection assays

GST-pERK (0.1 μ g) was incubated with 2 μ g vimentin or neurofilament (NF) for 2 h at 37 °C. Alkaline phosphatase (AP, two units, Roche, Mannheim, Germany) or axoplasm from injured nerve (100 μ g) was then added for an additional 30 min. Complexes were purified over GST beads followed by Western blot analysis for pERK. AP activity was verified with the synthetic substrate *p*-nitrophenyl phosphate (pNPP, Sigma cat. no. S0942) as described.¹⁴

ELISA

Recombinant GST-pErk (100 ng/well) or GST alone (45 ng/well) was immobilized on glutathione coated HS 96 well plates (Sigma) following the manufacturer's instructions. Vimentin and peptides were added in Tris-HCl buffer (pH 7.6) + CaCl₂ (10⁻⁶ M), and incubated at room temperature for 2 h, followed by three washes with Tris-HCl and two washes with PBS. Anti-vimentin monoclonal (Chemicon, 1:1000) was added and incubated at 4 °C overnight, followed by three washes with PBS. Goat anti-mouse HRP (BioRad) was then applied for a further 2 h at room temperature, reactions were developed with substrate after extensive washing, and scanned at 405 nm.

Acknowledgements

We thank Dr Robert Shoeman (MPI for Cell Biology) for the kind gift of vimentin and peripherin cDNAs. Supported by the Adelson Program in Neural Repair and Rehabilitation and the Minerva Foundation (to M.F.), and the Kimmelman Center for Biomolecular Structure and Assembly (to M.E.). R.S. holds the Yale S. Lewine and Ella Miller Lewine Professorial Chair for Cancer Research, and M.F. is the incumbent of the Chaya Professorial Chair in Molecular Neuroscience.

References

- Kolch, W. (2005). Coordinating ERK/MAPK signaling through scaffolds and inhibitors. *Nature Rev. Mol. Cell. Biol.* **6**, 827–837.
- Rubinfield, H. & Seger, R. (2005). The ERK cascade: a prototype of MAPK signaling. *Mol. Biotechnol.* **31**, 151–174.
- Yoon, S. & Seger, R. (2006). The extracellular signal-regulated kinase: multiple substrates regulate diverse cellular functions. *Growth Factors*, **24**, 21–44.
- Kholodenko, B. N. (2002). MAP kinase cascade signaling and endocytic trafficking: a marriage of convenience? *Trends Cell Biol.* **12**, 173–177.
- Kholodenko, B. N. (2003). Four-dimensional organization of protein kinase signaling cascades: the roles of diffusion, endocytosis and molecular motors. *J. Exp. Biol.* **206**, 2073–2082.
- Kholodenko, B. N. (2006). Cell-signalling dynamics in time and space. *Nature Rev. Mol. Cell. Biol.* **7**, 165–176.
- Cavalli, V., Kujala, P., Klumperman, J. & Goldstein, L. S. (2005). Sunday Driver links axonal transport to damage signaling. *J. Cell Biol.* **168**, 775–787.
- Sung, Y. J., Povelones, M. & Ambron, R. T. (2001). RISK-1: a novel MAPK homologue in axoplasm that is activated and retrogradely transported after nerve injury. *J. Neurobiol.* **47**, 67–79.
- Lindwall, C. & Kanje, M. (2005). Retrograde axonal transport of JNK signaling molecules influence injury induced nuclear changes in p-c-Jun and ATF3 in adult rat sensory neurons. *Mol. Cell. Neurosci.* **29**, 269–282.
- Ambron, R. T. & Walters, E. T. (1996). Priming events and retrograde injury signals—A new perspective on the cellular and molecular biology of nerve regeneration. *Mol. Neurobiol.* **13**, 61–79.
- Perlson, E., Hanz, S., Medzihradzky, K. F., Burlingame, A. L. & Fainzilber, M. (2004). From snails to sciatic nerve: retrograde injury signaling from axon to soma in lesioned neurons. *J. Neurobiol.* **58**, 287–294.
- Hanz, S., Perlson, E., Willis, D., Zheng, J. Q., Massarwa, R., Huerta, J. J. *et al.* (2003). Axoplasmic importins enable retrograde injury signaling in lesioned nerve. *Neuron*, **40**, 1095–1104.
- Perlson, E., Medzihradzky, K. F., Darula, Z., Munno, D. W., Syed, N. I., Burlingame, A. L. & Fainzilber, M. (2004). Differential proteomics reveals multiple components in retrogradely transported axoplasm after nerve injury. *Mol. Cell. Proteomics*, **3**, 510–520.
- Perlson, E., Hanz, S., Ben-Yakov, K., Segal-Ruder, Y., Seger, R. & Fainzilber, M. (2005). Vimentin-dependent spatial translocation of an activated MAP kinase in injured nerve. *Neuron*, **45**, 715–726.
- Herrmann, H., Haner, M., Brettel, M., Muller, S. A., Goldie, K. N., Fedtke, B. *et al.* (1996). Structure and assembly properties of the intermediate filament protein vimentin: the role of its head, rod and tail domains. *J. Mol. Biol.* **264**, 933–953.
- Herrmann, H. & Aebi, U. (2000). Intermediate filaments and their associates: multi-talented structural elements specifying cytoarchitecture and cytodynamics. *Curr. Opin. Cell Biol.* **12**, 79–90.
- Shoeman, R. L., Hartig, R., Berthel, M. & Traub, P. (2002). Deletion mutagenesis of the amino-terminal head domain of vimentin reveals dispensability of large internal regions for intermediate filament assembly and stability. *Exp. Cell Res.* **279**, 344–353.
- Rogers, K. R., Eckelt, A., Nimmrich, V., Janssen, K. P., Schliwa, M., Herrmann, H. & Franke, W. W. (1995). Truncation mutagenesis of the non-alpha-helical

- carboxyterminal tail domain of vimentin reveals contributions to cellular localization but not to filament assembly. *Eur. J. Cell Biol.* **66**, 136–150.
19. Klotzsche, O., Etzrodt, D., Hohenberg, H., Bohn, W. & Deppert, W. (1998). Cytoplasmic retention of mutant *tsp53* is dependent on an intermediate filament protein (vimentin) scaffold. *Oncogene*, **16**, 3423–3434.
 20. Canagarajah, B. J., Khokhlatchev, A., Cobb, M. H. & Goldsmith, E. J. (1997). Activation mechanism of the MAP kinase ERK2 by dual phosphorylation. *Cell*, **90**, 859–869.
 21. Strelkov, S. V., Herrmann, H., Geisler, N., Wedig, T., Zimbelmann, R., Aebi, U. & Burkhard, P. (2002). Conserved segments 1A and 2B of the intermediate filament dimer: their atomic structures and role in filament assembly. *EMBO J.* **21**, 1255–1266.
 22. Ben-Zeev, E., Kowalsman, N., Ben-Shimon, A., Segal, D., Atarot, T., Noivirt, O. *et al.* (2005). Docking to single-domain and multiple-domain proteins: old and new challenges. *Proteins: Struct. Funct. Genet.* **60**, 195–201.
 23. Rubinfeld, H., Hanoch, T. & Seger, R. (1999). Identification of a cytoplasmic-retention sequence in ERK2. *J. Biol. Chem.* **274**, 30349–30352.
 24. Tanoue, T., Adachi, M., Moriguchi, T. & Nishida, E. (2000). A conserved docking motif in MAP kinases common to substrates, activators and regulators. *Nature Cell Biol.* **2**, 110–116.
 25. Lee, T., Hoofnagle, A. N., Kabuyama, Y., Stroud, J., Min, X., Goldsmith, E. J. *et al.* (2004). Docking motif interactions in MAP kinases revealed by hydrogen exchange mass spectrometry. *Mol. Cell.* **14**, 43–55.
 26. Reszka, A. A., Bulinski, J. C., Krebs, E. G. & Fischer, E. H. (1997). Mitogen-activated protein kinase/extracellular signal-regulated kinase 2 regulates cytoskeletal organization and chemotaxis via catalytic and microtubule-specific interactions. *Mol. Biol. Cell*, **8**, 1219–1232.
 27. Eblen, S. T., Catling, A. D., Assanah, M. C. & Weber, M. J. (2001). Biochemical and biological functions of the N-terminal, noncatalytic domain of extracellular signal-regulated kinase 2. *Mol. Cell. Biol.* **21**, 249–259.
 28. Helfand, B. T., Chou, Y. H., Shumaker, D. K. & Goldman, R. D. (2005). Intermediate filament proteins participate in signal transduction. *Trends Cell Biol.* **15**, 568–570.
 29. Hanz, S. & Fainzilber, M. (2006). Retrograde signaling in injured nerve - the axon reaction revisited. *J. Neurochem.* **99**, 13–19.
 30. Wilsbacher, J. L. & Cobb, M. H. (2001). Bacterial expression of activated mitogen-activated protein kinases. *Methods Enzymol.* **332**, 387–400.

Edited by J. Karn

(Received 23 July 2006; received in revised form 13 September 2006; accepted 14 September 2006)

Available online 27 September 2006